CHAPTER 6

EMBANKMENT MODEL TESTS

6.1 General

The present chapter aims to shed some insight into the performance of an embankment supported on groups of end-bearing and floating geopolymer stabilized soil columns (GPSCs) in very soft clay under traffic loading conditions. A series of instrumented embankment model tests are conducted on groups of end-bearing and floating GPSCs in very soft clay with an undrained shearing strength of 5 kPa, subjected to static and cyclic loading conditions.

The excess-pore water pressure and vertical stress on GPSCs and the surrounding soil were monitored using a pore pressure transducer and earth pressure cells. The excess pore water pressure distribution and stress concentration ratio for the end-bearing and floating GPSCs-supported embankments under static and cyclic loading were measured. The failure pattern of the GPSCs was observed by investigating the deformed shape of the GPSCs after the completion of the model tests. An equation has been proposed based on the collected data from physical model tests to predict the ultimate bearing capacity of the GPSCs-supported embankments considering the A_r and l/h ratio. Furthermore, the study compares the static and cyclic behavior of GPSCs treated soft soil under embankment. The primary parameters examined include the loading type (static and cyclic), l/h ratio (end-bearing and floating GPSCs where h is the height of the bed and l is the length of the column), and area replacement ratio (A_r). The findings showed the relationship between the settlement response of the groups of GPSCs and these influencing parameters.

In addition, a life cycle assessment of geopolymer in comparison to OPC was performed, showing that geopolymer is a sustainable and eco-friendly construction material.

6.2 Test Conditions and Variables

In this study, the physical model tests simulate an embankment over a composite foundation with geopolymer columns installed vertically at a uniform spacing in a horizontal clay layer in the square pattern and subjected to vertical loading. Fourteen experiments were conducted on the unimproved and improved soft soil models with various area replacement ratios (A_r) and *l/h* ratios (end bearing and floating columns) and subjected to static and cyclic loading.

Table 6.1 provides the parameters adopted for the tests on unimproved and improved soft clay ground using floating and end-bearing geopolymer-treated soil columns (GPSCs). As a reference, static and cyclic loading tests were carried out on an unimproved soft clay bed with an undrained shear strength of 5 kPa. A total of twelve experiments, with six under static loading tests and six under cyclic loading conditions, were performed on the improved ground with different area replacement ratios and two-column lengths to the height of the soil bed ratios (*l/h*), including end-bearing and floating columns. The geopolymer column of 30 mm diameter and varying lengths (end-bearing and floating) are installed in a soft clay bed as per the test scheme.

The ratio of GGBS and dolomite was 80:20, and the NaOH: Na_2SiO_3 ratio was 25:75. The NaOH solution was prepared with molarity of 8M, and the alkali activator and binder ratio was 1. The binder content of 20% was mixed with the soil. The details of mixing geopolymer with soil are mentioned in the model preparation and column installation section of Chapter 3. The above geopolymer mix was found to provide

maximum strength. Therefore, the DSM column was constructed with optimum geopolymer as a binder.

Table 6.1 Summary of the parameters used in physical modeling.

Test no.	Test condition	l (mm)	Number of columns	A_r (%)	l/h	Loading pattern
1.	Unimproved	-	0	-	-	Static
2.	Unimproved	-	0	-	-	Cyclic
3.	End-bearing	240	9	12.7	1	Static
4.	End-bearing	240	12	17	1	Static
5.	End-bearing	240	15	21.2	1	Static
6.	Floating	180	9	12.7	0.75	Static
7.	Floating	180	12	17	0.75	Static
8.	Floating	180	15	21.2	0.75	Static
9.	End-bearing	240	9	12.7	1	Cyclic
10.	End-bearing	240	12	17	1	Cyclic
11.	End-bearing	240	15	21.2	1	Cyclic
12.	Floating	180	9	12.7	0.75	Cyclic
13.	Floating	180	12	17	0.75	Cyclic
14.	Floating	180	15	21.2	0.75	Cyclic

6.3 Results and Discussion

6.3.1 Response under Static Loading

6.3.1.1 Load-Settlement Behavior under Static Loading

Fig. 6.1 shows the vertical pressure-settlement response of the embankment model stabilized with end-bearing (l/h = 1) and floating (l/h = 0.75) GPSCs with area replacement ratios of 12.7%, 17%, and 21.2%. The results were compared with the untreated soil embankment model, which provides a reference for understanding the degree of improvement achieved after introducing the ground improvement technique.

As the settlement increases with increased applied pressure, the ultimate load intensity is considered at 50 mm settlement. This settlement was selected as a termination criterion for the experiments, as this was the maximum distance up to which the head of the load cell (connected to the actuator) could extend.

Compared to untreated soil, it was found that the ultimate vertical stress and the stiffness of the embankment model ground increase with the installation of end-bearing or floating columns. The ground improved with end-bearing GPSCs showed better performance than floating columns as they can mobilize high end-bearing stresses. The stress-settlement curves in Fig. 6.1 showed that the untreated soil shows local shear failure with some heaving around the loading area. With the installation of columns, general shear failure was observed for both end-bearing columns (l/h = 1) and floating columns (l/h = 0.75). The ultimate bearing capacity obtained for untreated soil was 25 kPa. On comparing the ultimate bearing capacity (q_{ult}) at 50 mm settlement for the embankment model on soft clay improved with GPSCs, the highest q_{ult} was obtained at an area replacement ratio of 21.2% and l/h = 1, and minimum q_{ult} was recorded at area replacement ratio of 12.7% and l/h = 0.75.

It was found that the q_{ult} of the embankment model installed with GPSCs increased with an increase in A_r and l/h ratio, which shows good agreement with previously reported studies on soil-cement columns installation in soft soil (Mat Said et al. 2019; Mohanty and Shahu 2021; Rashid et al. 2015). The increase in the area replacement ratio increases the stiffness and ultimate bearing capacity of the ground, and the ground tends to support higher vertical stresses. For l/h = 1, the q_{ult} increased by 246.92%, 344.56%, and 418.8%, and for l/h = 0.75, the increase in q_{ult} was 126.9%, 151% and 181.64% as compared to untreated soil for A_r of 12.7%, 17%, and 21.2% respectively. With an increase in A_r, the spacing between the columns is reduced, and the cross-

sectional area of the GPSCs is increased, which results in better performance of the embankment model over improved kaolin clay.

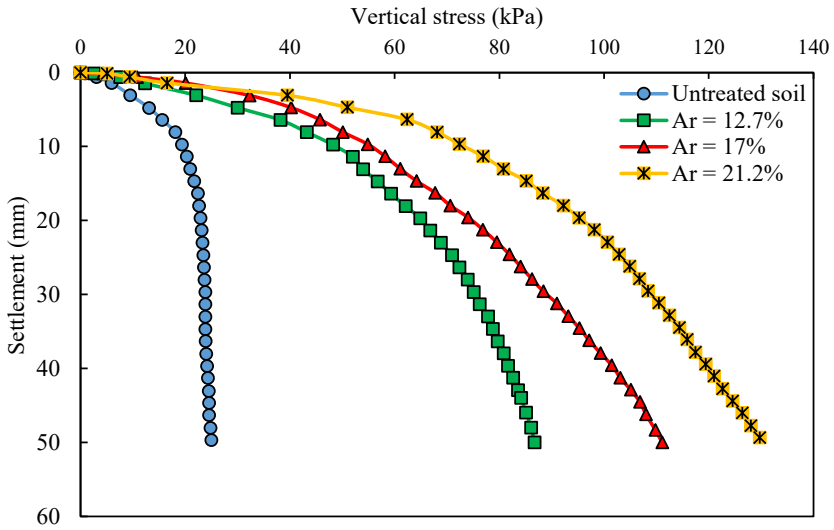

(a)

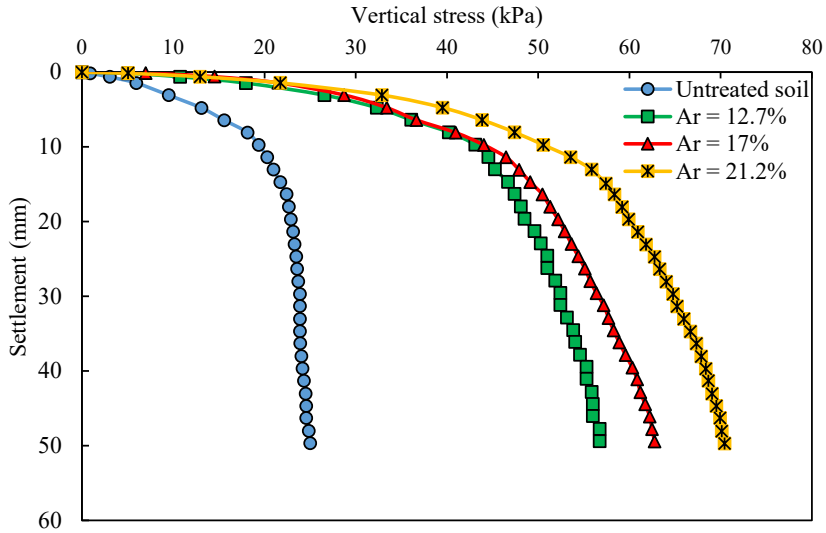

(b)

Fig. 6.1 Applied vertical stress against footing settlement behavior for the unimproved and GPSCs improved embankment model with A_r of 12.7%, 17%, and 21.2% (a) End-bearing GPSCs (l/h = 1) and (b) Floating GPSCs (l/h = 0.75).

6.3.1.2 Response of Excess Pore Water Pressure under Static Loading

Fig. 6.2 shows the influence of A_r and l/h on excess pore water pressure response under static embankment loading conditions. The excess pore pressure response of the untreated embankment model was also obtained. It was observed that the excess pore water pressure was increasing with applied vertical stress, and the peak excess pore water pressure (P_{max}) of 17.3 kPa was obtained for the untreated soil model. With the application of GPSCs, a smaller excess pore water pressure response was observed. The P_{max} for the A_r of 12.7%, 17%, and 21.2% was 6.38 kPa, 5.88 kPa, 2.71 kPa for l/h =1, and 11.93 kPa, 7.23 kPa, and 3.47 kPa for l/h = 0.75 respectively. It was observed that the installation of GPSCs significantly reduced the P_{max} value compared to untreated soil, and the reduction in P_{max} was higher for end-bearing GPSCs compared to floating GPSCs. Additionally, the increase in A_r helps in reducing the P_{max} value because with an increase in A_r, the number of GPSCs increases, which takes a higher load than the surrounding soil. As the stress on the surrounding soil reduces, the excess pore water pressure reduces.

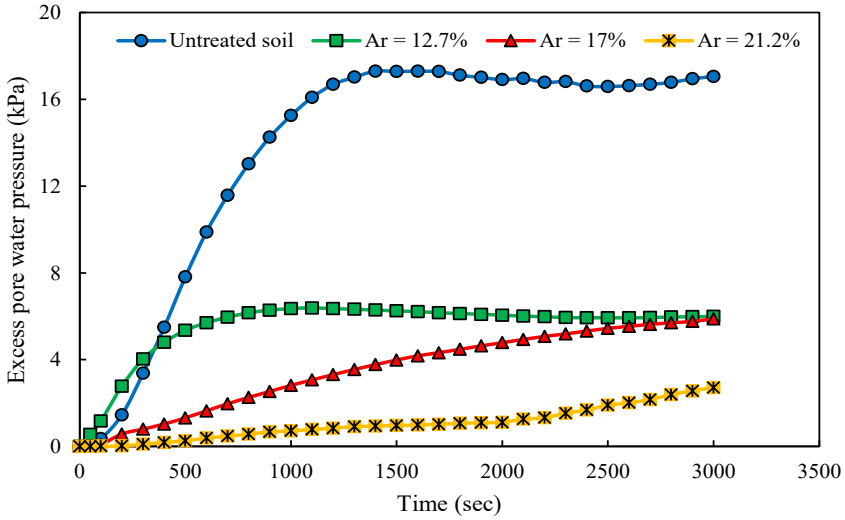

(a)

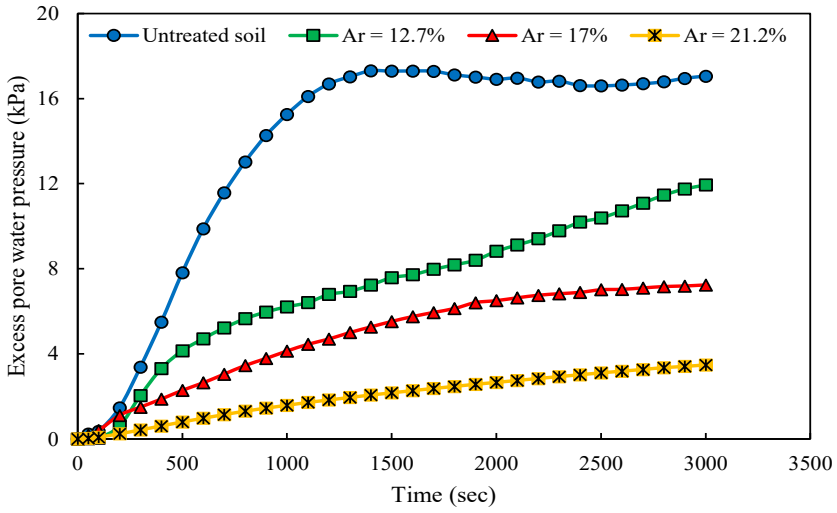

(b)

Fig. 6.2 Variation of excess pore water pressure with time for the unimproved and GPSCs improved embankment model with A_r of 12.7%, 17%, and 21.2% (a) End-bearing GPSCs (l/h = 1) and (b) Floating GPSCs (l/h = 0.75).

6.3.1.3 Effect of Static Loading on the Stress Concentration Ratio

Fig. 6.3 shows the stresses acting on top of the surrounding soil and GPSCs under static loading conditions for different A_r and l/h ratios. The stress on the surrounding soil and GPSCs increases with vertical stress. For both l/h =1 and l/h = 0.75, the stress on surrounding soil is reduced, and the stress on GPSCs is increased with an increase in A_r. The maximum stress of 55.75 kPa and 53.5 kPa for A_r of 12.7% and minimum stress of 43.63 kPa and 38 kPa for A_r of 21.2% were obtained on the surrounding soil for l/h = 1 and l/h = 0.75 respectively. Although the stress acting on the surrounding soil was around the same for both l/h ratios, the stress acting on the column was significantly different. The stress on the column was higher for an l/h ratio of 1, i.e., the end-bearing column, than the floating column with an l/h ratio of 0.75 for all area replacement ratios. For an l/h = 1, the stress on the column was 165.5 kPa, 200.77 kPa, and 310.45 kPa, whereas, for l/h = 0.75, the stress on the column was 86.9 kPa, 93.91 kPa, and 102 kPa

for A_r of 12.7%, 17%, and 21.2% respectively. Hence, it can be concluded that the stress on the column increases with an increase in A_r and l/h ratios.

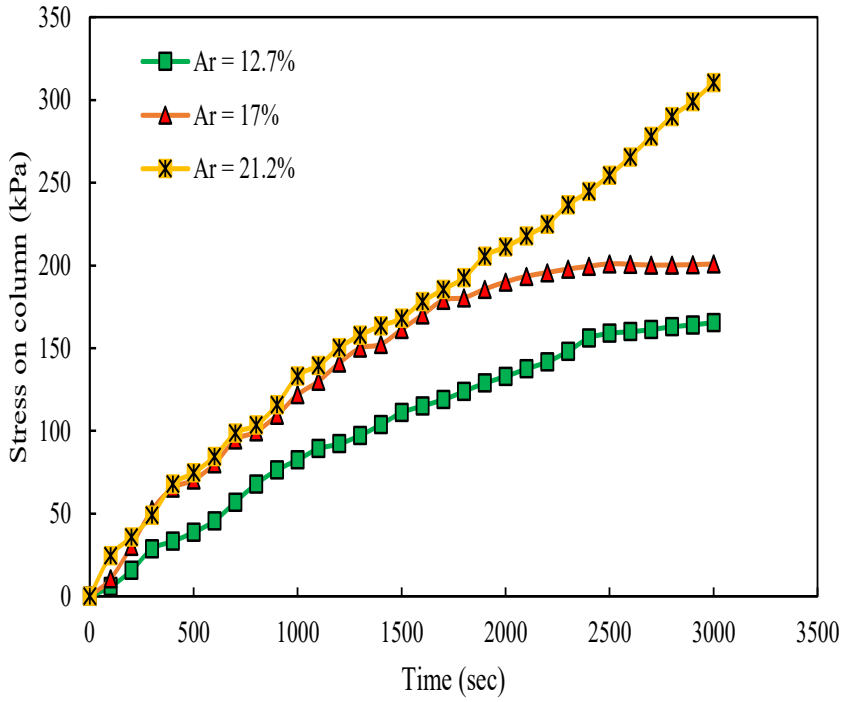

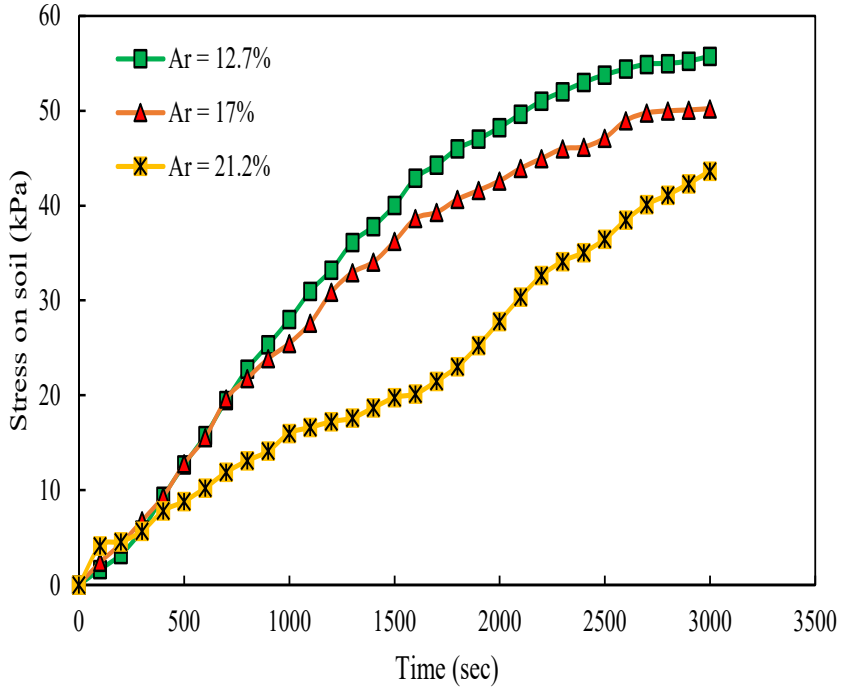

(a)

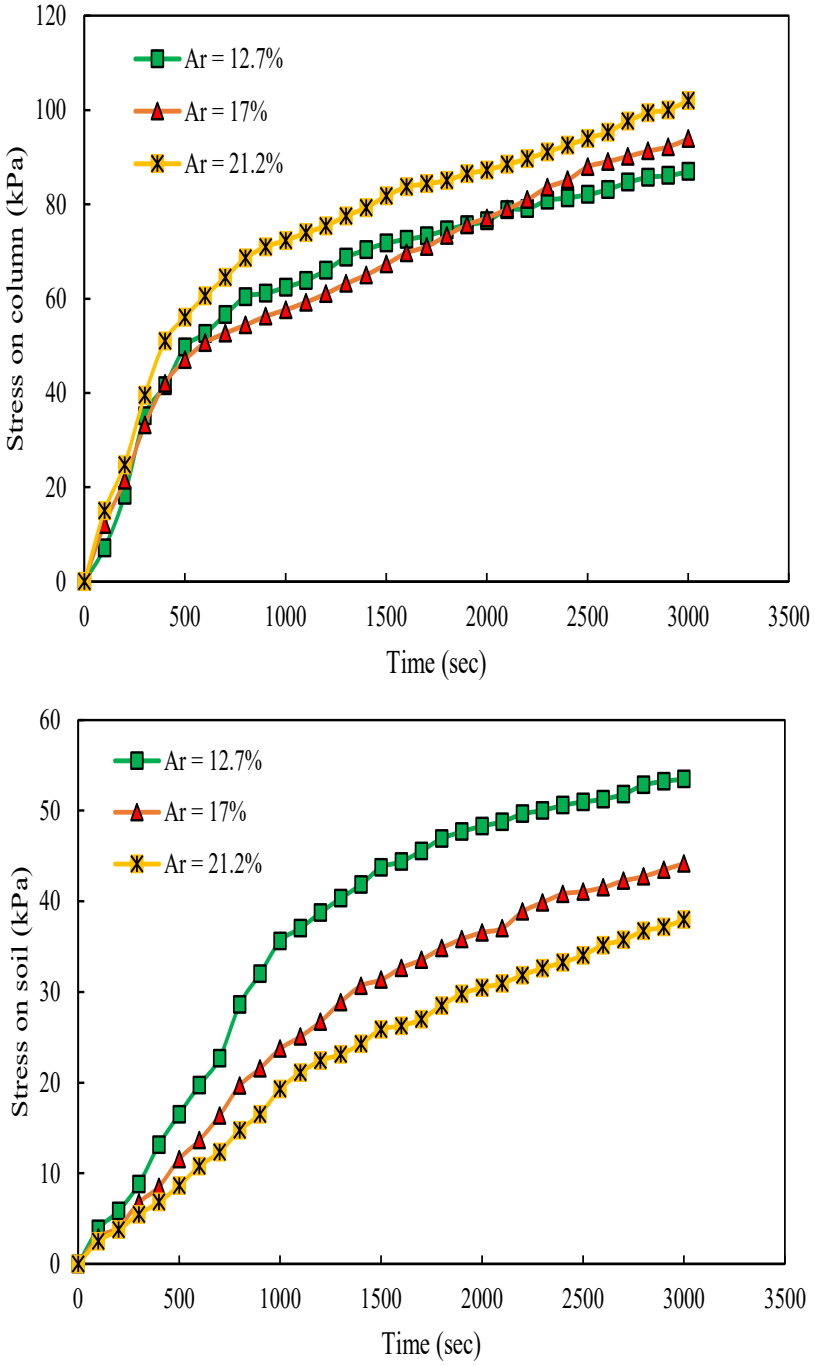

(b)

Fig. 6.3 Stress acting on column and soil under static embankment loading (a) End-bearing GPSCs (l/h = 1) and (b) Floating GPSCs (l/h = 0.75).

The stress concentration ratio (SCR) is defined as the ratio of stress acting on the column to the stress acting on the soil. SCR greater than 1 indicates that the column takes the higher stress during embankment loading, and the stress is transferred from the surrounding soil to the column, whereas SCR less than 1 indicates the load transfer from the column to the surrounding soil (Yun-min et al. 2008). The SCR depends on various factors such as column stiffness, soil properties, loading rate, area replacement ratio, *l/h* ratio, etc.

Fig. 6.4 shows the curve of SCR with time for end-bearing and floating columns with different area replacement ratios. The curve of SCR was found to increase with time, attain a peak value, and then start to decrease gradually, attaining an almost steady value indicating a loss in maximum arching after a certain time. Previous studies on the column-supported embankment have also reported similar findings (Han and Gabr 2002; Zhao et al. 2023). It was found that SCR increases with an increase in A_r, i.e., as the column spacing reduces, the SCR value increases. Also, SCR for end-bearing GPSCs (i.e., l/h = 1) was higher than floating GPSCs (i.e., l/h = 0.75). The maximum SCR was obtained for the embankment model with A_r = 21.2% and l/h =1, and the minimum SCR was obtained for A_r = 12.7% and l/h = 0.75, indicating that with an increase in the number of columns and length of columns, the load transferred to the column is higher.

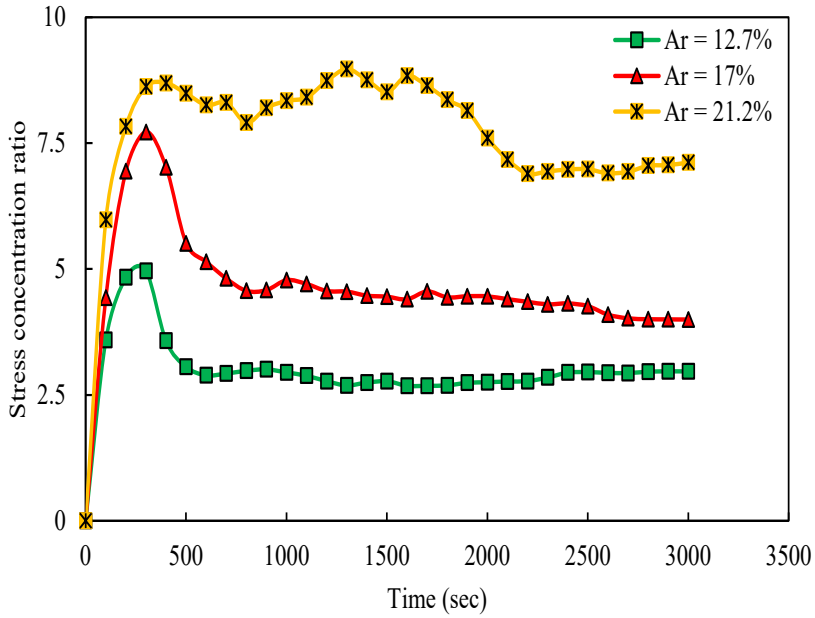

(a)

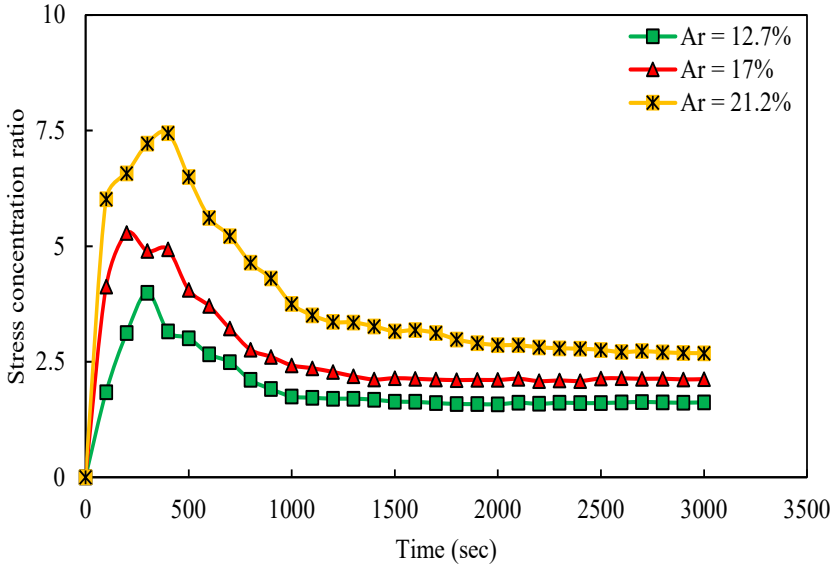

(b)

Fig. 6.4 Variation of stress concentration ratio under static embankment loading (a) End-bearing GPSCs (l/h = 1) and (b) Floating GPSCs (l/h = 0.75).

6.3.1.4 Ultimate Bearing Capacity of Soft Soil Treated with GPSCs

As per the ultimate failure load criterion, the ultimate failure load is defined as a point at which the slope of the load-settlement curve first approaches zero or reaches a stable, minimal value. As the load was found to be increasing with settlement for end-bearing columns, the failure stress at 50 mm settlement is considered the ultimate load (q_{ult}). A bearing capacity factor term was used to do the test comparison, accounting for slight variations in the undrained shear strength of the soil (Bouassida and Porbaha 2005). The bearing capacity factor is determined using the following Eq. (6.1).

$$N_c = \frac{q_{ult}}{c_{us}} \tag{6.1}$$

where c_{us} is the undrained shear strength of the soft soil in the model test. As shown in Fig. 6.5, the relationship between N_c and A_r was polynomial non-linear for both end-bearing and floating columns. Rashid et al. (2017), Moradi et al. (2019), etc., achieved a similar relationship for the model ground improved with soil-cement columns. The bearing capacity of the untreated embankment model was found to be 5, which is a little less than the theoretical bearing capacity factor of 5.14 for rectangular foundations on clay. The N_c value was higher for end-bearing columns treated embankment model, and the N_c value was found to be increasing with an increase in A_r. The N_c values obtained for end-bearing and floating GPSCs were compared, and the bearing improvement ratio was determined. The bearing improvement factor (BIF) is determined as the ratio of the bearing capacity of the column-treated model ground to that of the untreated model ground. All the results of the embankment model tests are summarized in Table 6.2. It was found that the BIF for floating columns ranged between 2.19 and 2.79, whereas for end-bearing columns, it ranged between 3.32 to 5.09.

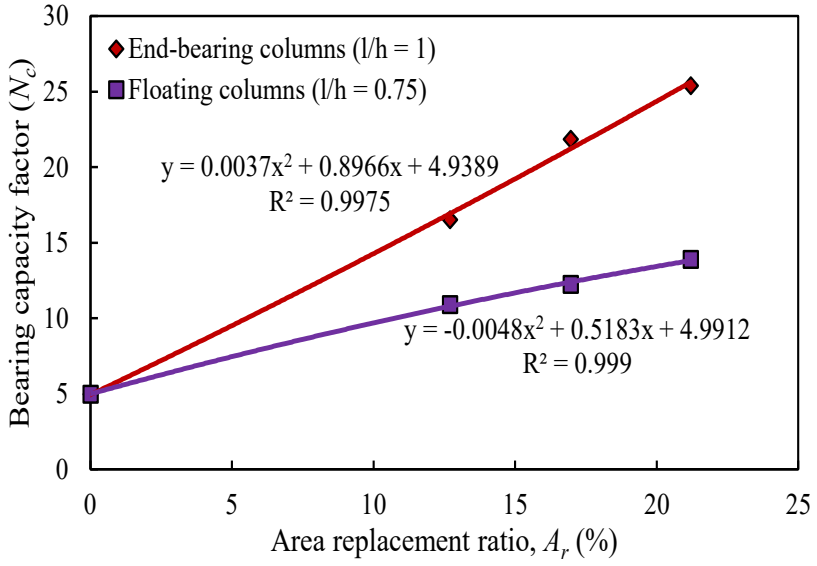

Fig. 6.5 Relationship between N_c and A_r for the embankment model improved with end-bearing and floating GPSCs.

Table 6.2 Summary of the test results of the embankment model under static loading.

Model test	A_r (%)	*l/h*	Failure stress, q_{ult} (kPa)	N_c	Bearing improvement factor (BIF)
Untreated soil	-	-	25.1	5	-
End-bearing columns	12.7	1	86.73	16.52	3.32
End-bearing columns	17	1	111.14	21.83	4.38
End-bearing columns	21.2	1	129.7	25.38	5.09
Floating columns	12.7	0.75	56.73	10.91	2.19
Floating columns	17	0.75	62.46	12.23	2.45
Floating columns	21.2	0.75	70.41	13.89	2.79

For design purposes, estimating N_c on the improved ground is challenging. Although the expressions of N_c for the DSM-treated ground under rigid footing have been developed considering area replacement ratios (Moradi et al. 2019; Rashid et al.

2015), the expression considering both area replacement ratio and length of the column under embankment loading is rarely available. A general expression of N_c was developed based on physical model tests for GPSCs improved soil under the embankment with variation in A_r and l/h ratio, given in Eq. (6.2). The approximate values of N_c with l/h and A_r using the above equation are shown in Fig. 6.6. The correlation coefficient of 0.99 was achieved in the above equation. The equation validates the A_r range of 12.7% to 21.2%, the l/h ratio of 0.75 to 1.

$$N_c = -0.02{A_r}^2 + 2.77\, A_r.{}^{l}/_{h} - 11.34\,{}^{l}/_{h} - 1.06A_r + 9.54 \qquad (6.2)$$

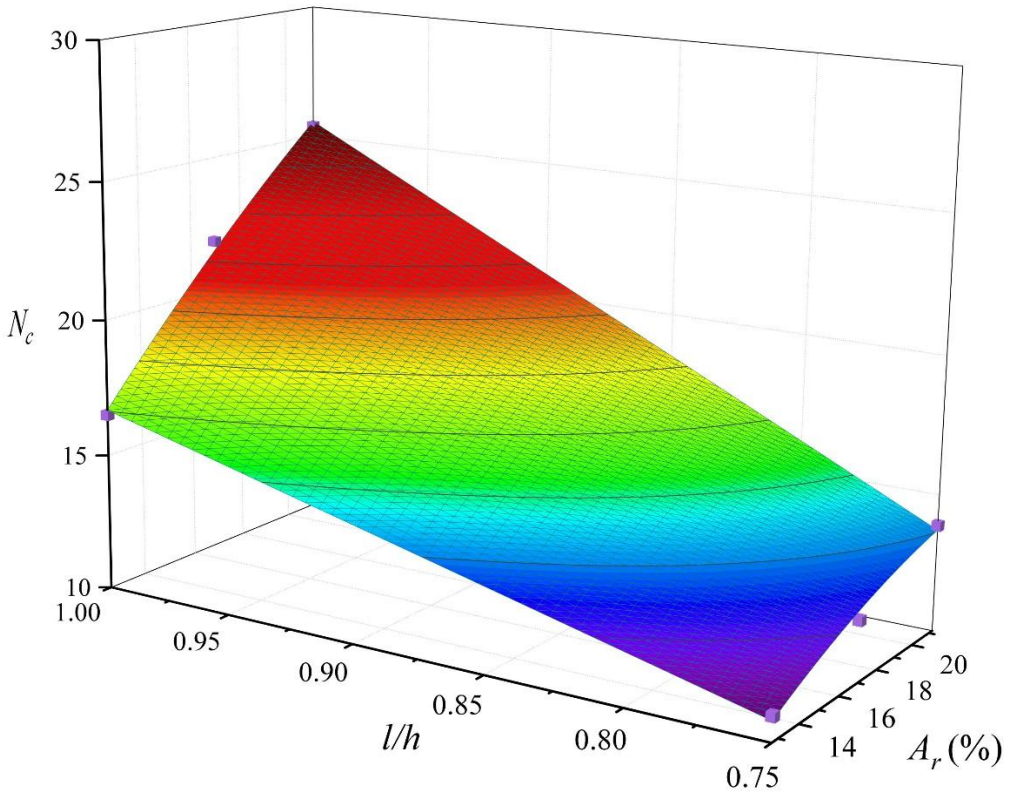

Fig. 6.6 Variation of N_c against different l/h ratios and A_r.

6.3.1.5 Failure Pattern of Soft Soil Treated with GPSCs under Static Loading

After completion of each of the experiments, the failure pattern of the embankment model was inspected. Fig. 6.7 displays the typically improved ground failure patterns for all the experiments under static loading. Fig. 6.7 (a-c) shows the failure patterns of end-bearing GPSCs, and Fig. 6.7 (d-e) shows the pattern of floating GPSCs under static loading. Only the second row is considered and displayed for both end-bearing and floating columns, as the failure mechanism of the columns in all the rows was almost identical. Since the columns failed one at a time during the loading rather than all at once, the variation in the failure modes in the row of soil slices may be related to the progressive failure in the group of columns. For the end-bearing case, the GPSCs falling under the crest part showed shear failure, whereas the GPSCs falling under the slope part failed due to bending. At A_r of 12.7% and l/h = 1, the column under the crest area had a shear failure, and the columns under the slope area were slightly moved outwards. It can be due to the large spacing between the columns, so the other columns do not participate in taking the vertical stress, which can also be the reason for lower ultimate bearing capacity. With the increase in A_r, spacing between columns reduces, so the columns under the slope area also participate in taking the vertical stress and bent outwards, thus increasing the ultimate bearing capacity. In the case of floating GPSCs, punching failure along with slight outward movement of GPSCs were observed as the columns under the crest area penetrated vertically downwards. Some horizontal cracks were also observed in the GPSCs. In addition to this, the columns under the slope have a slight outward bending. The reason could be the higher strength of the columns compared to the surrounding soil which allowed the punching of the columns.

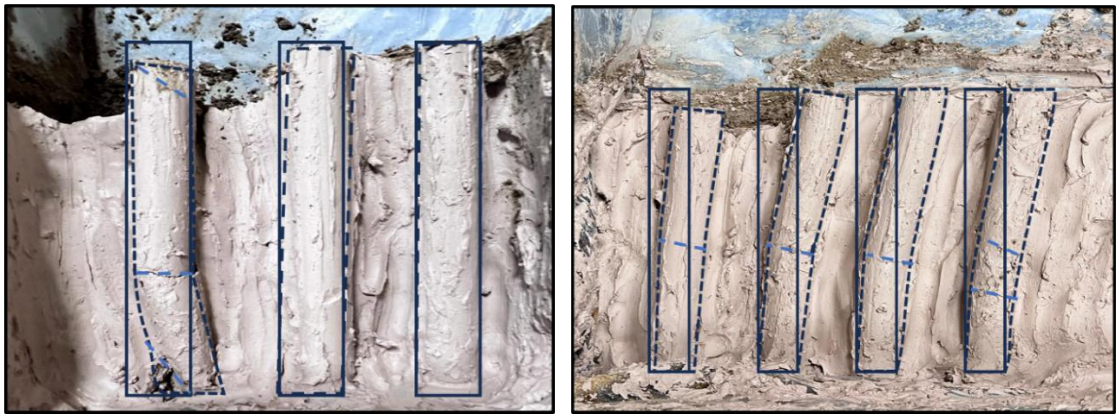

(a) (b)

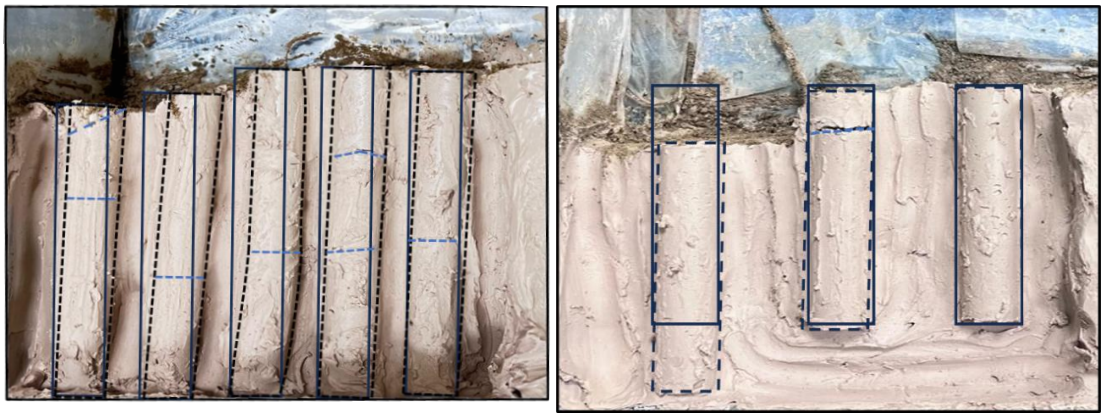

(c) (d)

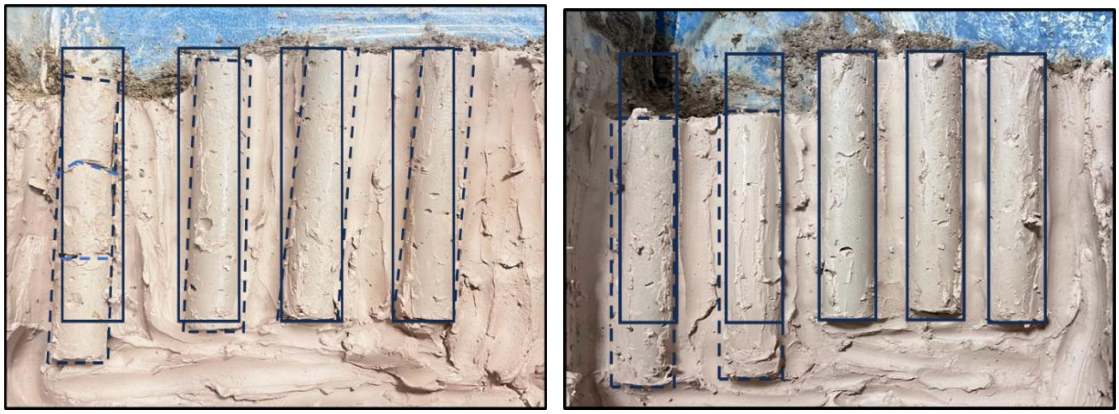

(e) (f)

Fig. 6.7 Settlement behavior of GPSCs under static embankment loading: end-bearing (l/h = 1) – (a) A_r = 12.7%, (b) A_r = 17%, (c) A_r = 21.2%; floating (l/h = 0.75) – (d) A_r = 12.7%, (e) A_r = 17%, and (f) A_r = 21.2%.

6.3.2 Response under Cyclic Loading

6.3.2.1 Load-Settlement Behavior under Cyclic Loading

Fig. 6.8 shows the plots obtained for the settlement values with the number of cycles under cyclic loading at A_r of 12.7%, 17%, and 21.2% for both *l/h* of 1 and 0.75. A cyclic loading test was also performed on the untreated soil embankment model to determine the degree of improvement. It was observed that under cyclic vertical pressure of 55 kPa, the untreated soil reached a 50 mm settlement within 300 cycles. With the inclusion of GPSCs, the induced settlement was reduced. For an *l/h* ratio of 1, it was observed that the settlement increases rapidly within the first few cycles, and after that, it reaches a stable value up to 10,000 cycles. With an increase in A_r from 12.7% to 17%, the settlement reduced from 18.58 mm to 14.34 mm, and with a further increase in A_r, reduced settlement to 8.94 mm in 10,000 cycles. The settlement was reduced by 22.82% and 37.65%, with respect to A_r of 17% and 21.2% compared to A_r of 12.7%.

For an *l/h* ratio of 0.75, the settlement was less than the untreated embankment model and higher as compared to the *l/h* ratio of 1 for the same A_r. For A_r of 12.7%, the embankment model reached 47.74 mm within 10,000 cycles. The increase in A_r to 17% significantly reduced settlement to 24.05 mm, and a further increase in A_r to 21.2% reduced the settlement to 14.65 mm. The reduction in settlement was 49.62% and 39.08%, with an increase in A_r from 12.7% to 17% and 21.2%, respectively. It was observed that the settlement for an *l/h* ratio of 1 and A_r of 17% was around the same for an *l/h* ratio of 0.75 and A_r of 21.2%. From the results, it can be concluded that under cyclic loading, floating columns with higher A_r showed a similar response as end-bearing columns with lower A_r, so in the case of floating columns, higher A_r is required.

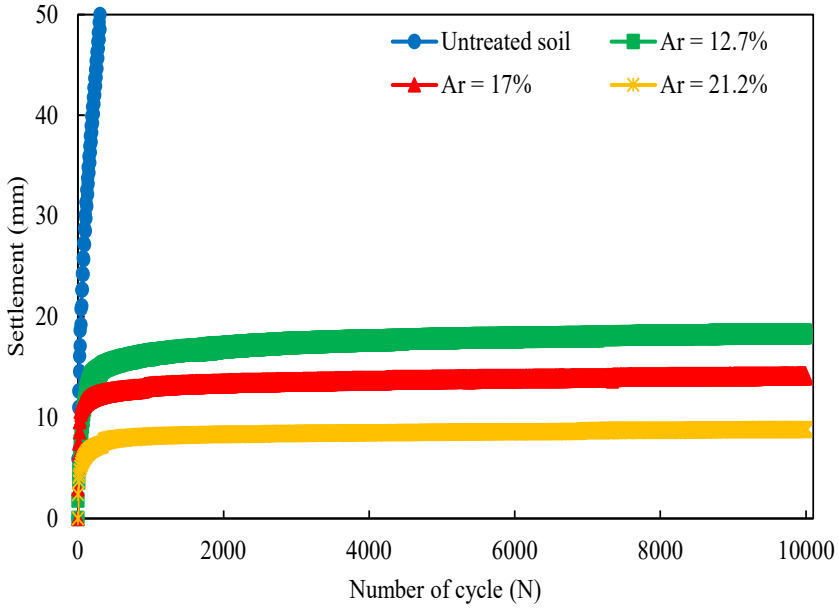

(a)

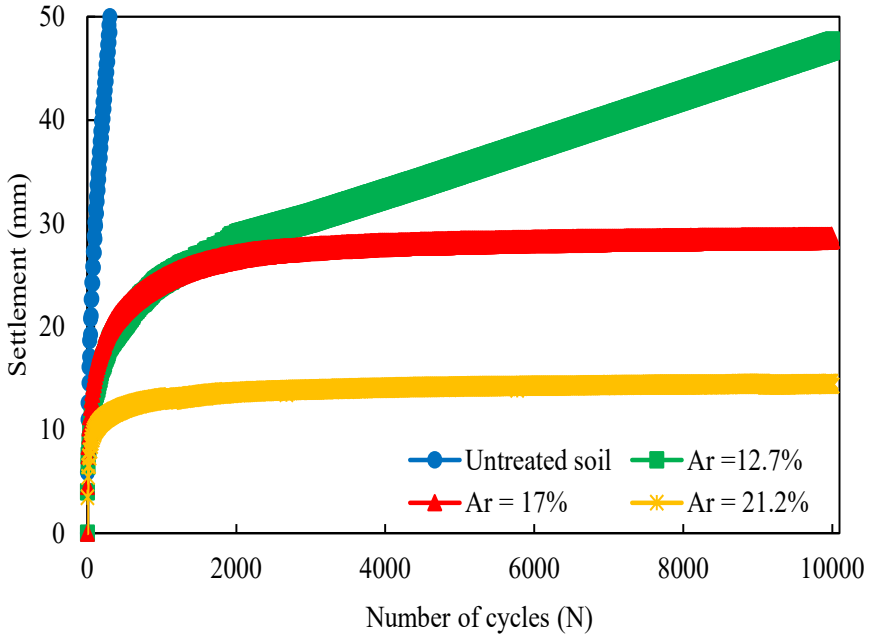

(b)

Fig. 6.8 Footing settlement with the number of load cycles for the unimproved and GPSCs improved embankment model with A_r of 12.7%, 17%, and 21.2% (a) End-bearing GPSCs (l/h = 1) and (b) Floating GPSCs (l/h = 0.75).

6.3.2.2 Response of Excess Pore Water Pressure under Cyclic Loading

Excess pore water pressure response was obtained to understand the influence of A_r and l/h ratio on the embankment model under cyclic loading, as shown in Fig. 6.9. The excess pore water pressure (P_{max}) of the untreated embankment model was 2.78 kPa at 50 mm settlement, which failed in 300 cycles. The excess pore water pressure trend was increasing in the untreated embankment model. With the inclusion of GPSCs, the excess pore water pressure decreased. The P_{max} for the A_r of 12.7%, 17%, and 21.2% was 3.99 kPa, 2.61 kPa, 1.872 kPa for l/h =1, and 7.58 kPa, 5.53 kPa, and 2.83 kPa for l/h = 0.75 respectively.

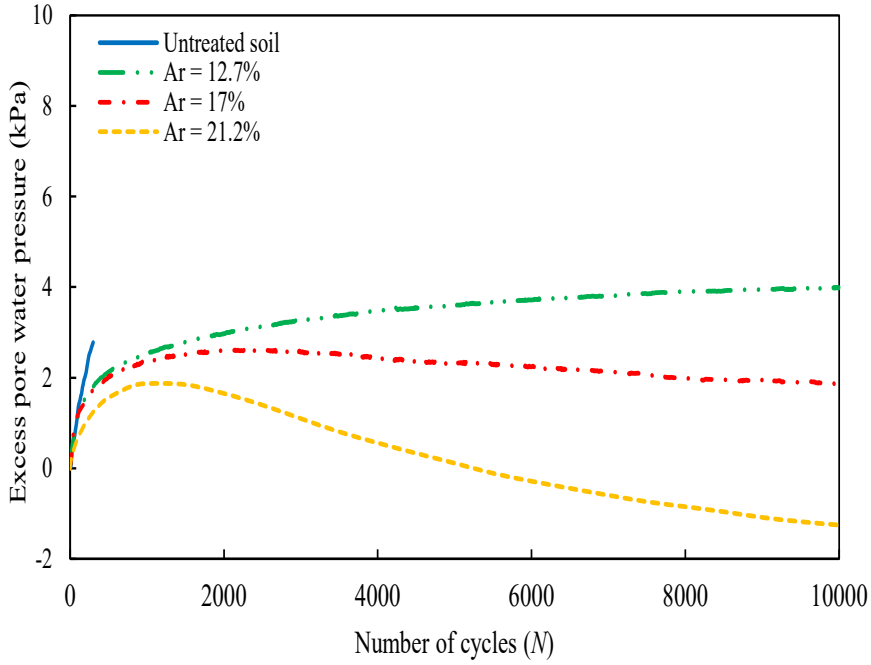

(a)

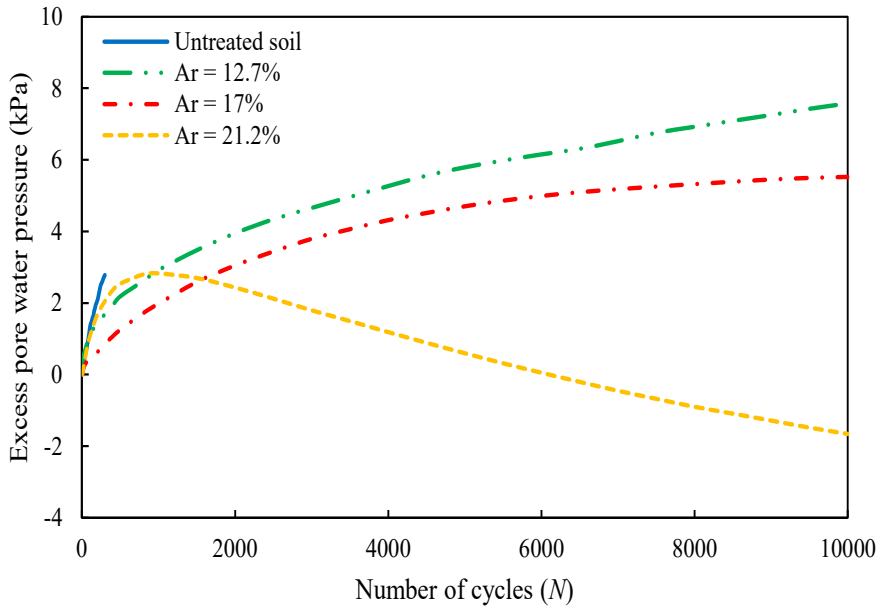

(b)

Fig. 6.9 Variation of excess pore water pressure with time under cyclic embankment loading for the unimproved and GPSCs improved embankment model with A_r of 12.7%, 17%, and 21.2% (a) End-bearing GPSCs (l/h = 1) and (b) Floating GPSCs (l/h = 0.75).

The excess pore water pressure was found to be decreasing with an increase in the A_r and l/h ratio. With an increase in A_r, GPSCs take a higher stress, and the stress on the surrounding soil is reduced, which is the reason for the reduction in P_{max} with an increase in A_r. In the case of A_r of 21.2 %, the excess pore water pressure increased for the first few cycles and gradually started to decrease and became negative with the number of cycles. The reason could be due to an increase in A_r; the cross-sectional area of the columns increased, and the surrounding soil decreased, which consequently led to a decrease in the volume of voids in the soil. Also, higher stress is taken by GPSCs; as a result, less stress is transferred to the surrounding soil. As the soil volume and soil stress are reduced, less excess pore water pressure is generated. With repeated cyclic loading, excess pore water pressure increases to its peak value in a few loading cycles.

Further increase in loading cycles results in the reduction of excess pore water pressure, which goes to negative due to less generation of excess pore water pressure.

6.3.2.3 Effect of Cyclic Loading on the Stress Concentration Ratio

Fig. 6.10 shows the variation of SCR with the number of cycles for different A_r and l/h ratios under cyclic loading. For all the cases, the SCR increases quickly within the first few cycles and then attains a constant value. A similar observation was found in the case of static loading. In the case of static loading, stress increases with time, whereas in cyclic loading case, a particular stress is applied for 10,000 cycles. The pattern of SCR was the same for static and cyclic loading. SCR value after 10,000 cycles for A_r of 12.7%, 17%, and 21.2% was 2.64, 5.13, and 7.59, respectively, whereas in the case of l/h = 0.75, SCR was 1.8, 3.09, and 3.65 for A_r of 12.7%, 17%, and 21.2% respectively. Higher SCR means higher stress is transferred to the GPSCs than the surrounding soil. With the increase in A_r and l/h, the settlement reduces, and SCR increases.

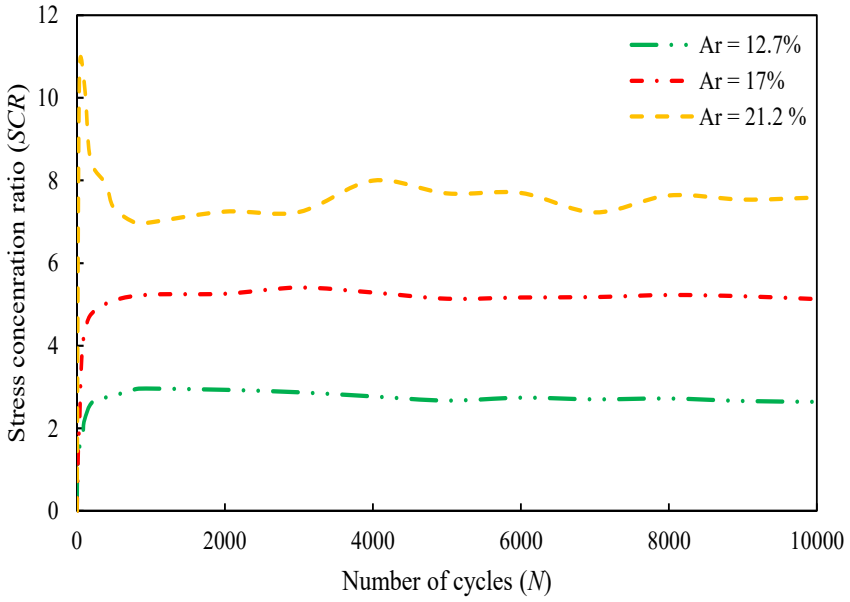

(a)

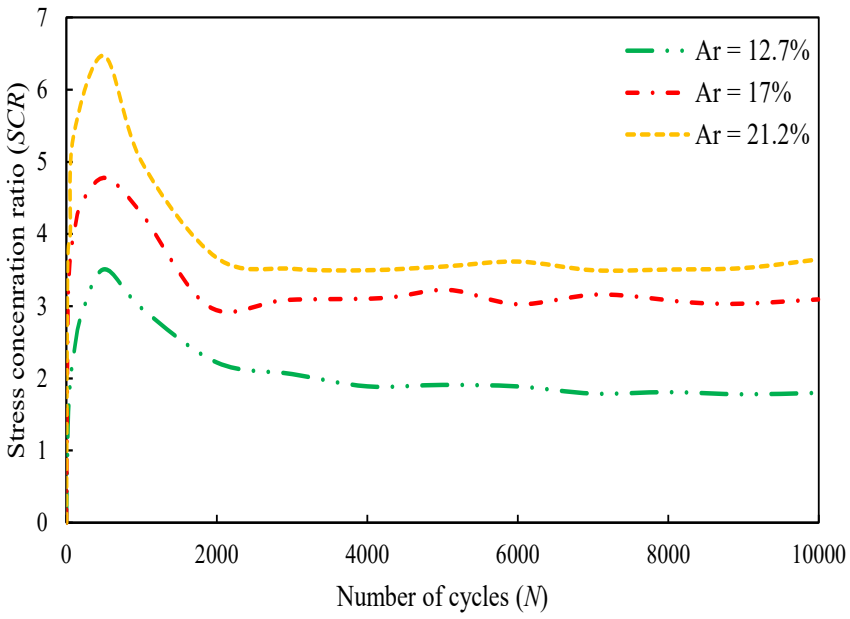

(b)

Fig. 6.10 Variation of stress concentration ratio under cyclic embankment loading (a) End-bearing GPSCs (l/h = 1) and (b) Floating GPSCs (l/h = 0.75).

6.3.2.4 Failure Pattern of Soft Soil Treated with GPSCs under Cyclic Loading

The failure pattern of GPSCs under cyclic embankment loading was observed with a change in the A_r and l/h ratio. Fig. 6.11 (a-c) shows the failure patterns of end-bearing GPSCs, and Fig. 6.11 (d-f) shows the pattern of floating GPSCs under cyclic loading. For the end-bearing case, the GPSCs falling under the crest part showed shear failure, whereas the GPSCs falling under the slope part failed due to bending. The outward movement of columns was less in cyclic loading as the settlement under the cyclic stress of 55 kPa was lower. In the case of floating GPSCs, punching failure of the columns was observed, which is the same as under static loading. Some horizontal cracks were also observed in the GPSCs. Punching with significantly less settlement was observed at l/h = 1 and A_r = 21.2%. A higher A_r of 21.2% in floating GPSCs showed better performance than end-bearing GPSCs with A_r = 12.7%.

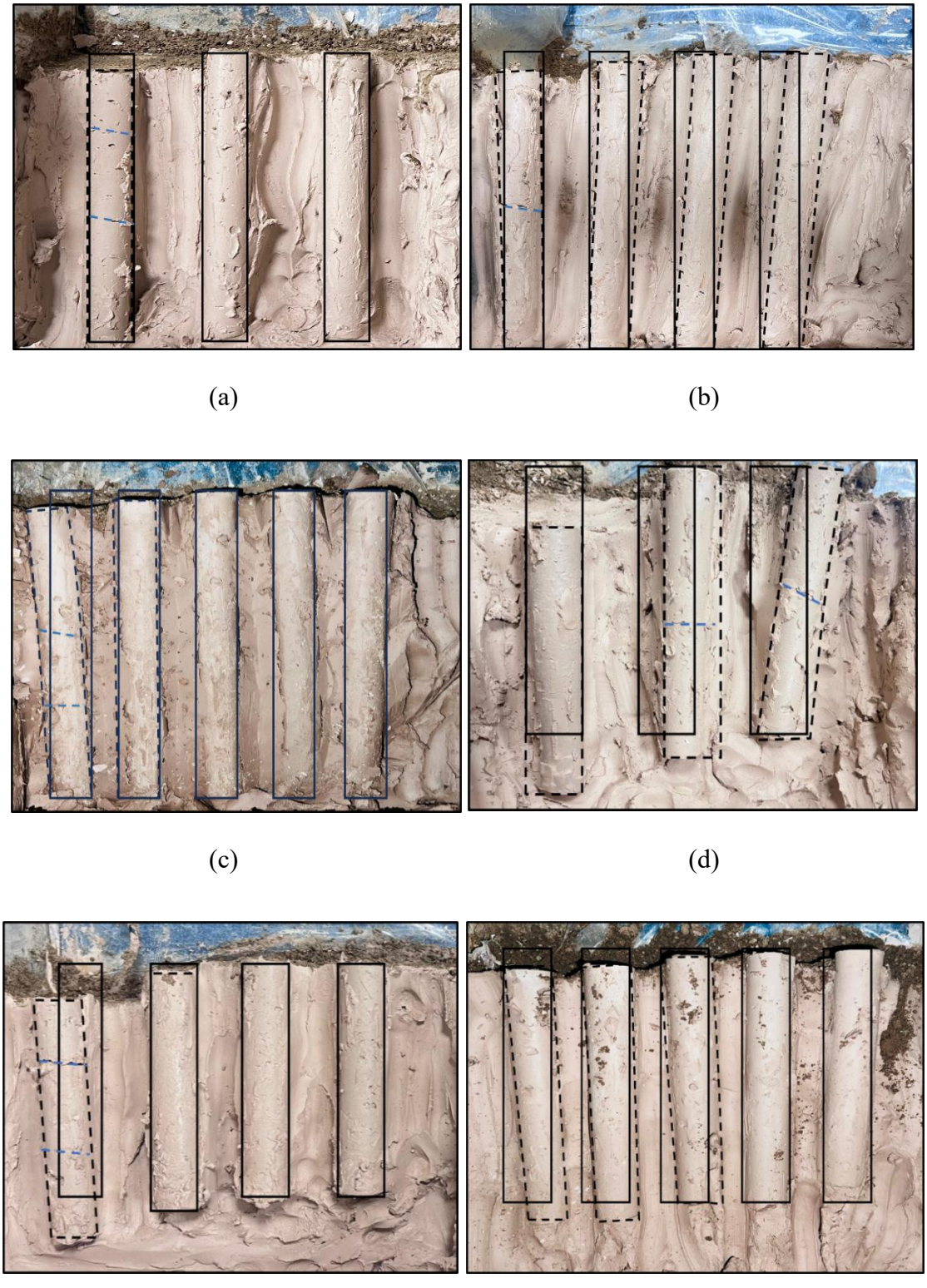

Fig. 6.11 Settlement behavior of GPSCs under cyclic embankment loading: end-bearing (l/h = 1) – (a) A_r = 12.7%, (b) A_r = 17%, (c) A_r = 21.2%; floating (l/h = 0.75) – (d) A_r = 12.7%, (e) A_r = 17%, and (f) A_r = 21.2%.

6.3.2.5 Settlement Response under Cyclic Loading vs. Static Loading

The measured cyclic settlement was compared with static cyclic settlement, and the results are presented in Table 6.3. In Table 6.3, $\delta_{static55}$ is the settlement corresponding to 55 kPa stress under static loading, δ_{static} is the total settlement reached at failure under static loading, and $\delta_{cyclic55}$ indicates the cyclic settlement reached at cyclic stress of 55 kPa in 10,000 cycles. The number multiplier by which the settlement under cyclic loading ($\delta_{cyclic55}$) surpasses the settlement under static loading ($\delta_{static55}$) is presented by $\delta_{cyclic55}/\delta_{static55}$ ratio. The $\delta_{cyclic55}/\delta_{static}$ ratio indicates the fraction of settlement under cyclic vertical stress of 55 kPa in 10,000 cycles to the total settlement reached on failure under static loading; in other words, this ratio represents how close the embankment model is to failure under cyclic loading.

Table 6.3 Comparison of settlement response of embankment model under static loading with cyclic loading.

Type of test	***l/h* ratio**	***A_r (%)***	**$\delta_{static55}$ (mm)**	**$\delta_{cyclic55}$ (mm)**	**δ_{static} (mm)**	$\frac{\delta_{cyclic55}}{\delta_{static55}}$	$\frac{\delta_{cyclic55}}{\delta_{static}}$
End-bearing columns	1	12.7	13.67	18.58	50	1.36	0.37
	1	17	9.76	14.34	49.4	1.47	0.29
	1	21.2	5.29	8.94	50	1.68	0.17
Floating columns	0.75	12.7	38.75	47.74	49.5	1.23	0.96
	0.75	17	26.01	28.86	49.3	1.11	0.58
	0.75	21.2	12.42	14.65	49.7	1.18	0.29

The results indicate that settlement under cyclic vertical stress of 55 kPa of the end-bearing GPSCs improved embankment model is 1.36 to 1.68 times greater than the settlement under static loading at vertical stress of 55 kPa. In the case of soft soil improved with floating GPSCs, the ratio varies from 0.92-1.23. Thus, the cyclic loading resulted in higher settlement as compared to static loading under the same magnitude of vertical stress.

A bar chart is plotted in Fig. 6.12 to better understand the comparison of static and cyclic loading. It was observed that the settlement under cyclic loading was less than the total failure settlement under static loading. In the case of l/h = 0.75 and A_r = 12.7%, $\delta_{cyclic55}/\delta_{static}$ is 0.96, indicating that cyclic stress of 55 kPa is enough to induce the failure settlement corresponding to static loading. The $\delta_{cyclic55}/\delta_{static}$ ratio for an l/h ratio of 1 and A_r of 17% was around the same for an l/h ratio of 0.75 and A_r of 21.2%, which shows that under cyclic loading, higher A_r floating GPSCs showed a similar response as lower A_r end-bearing GPSCs. From this observation, it can be concluded that in the case of floating GPSCs, a higher area replacement ratio is required for better load bearing under static and cyclic loading. Also, end-bearing GPSCs are comparatively more effective in the settlement reduction during cyclic loading.

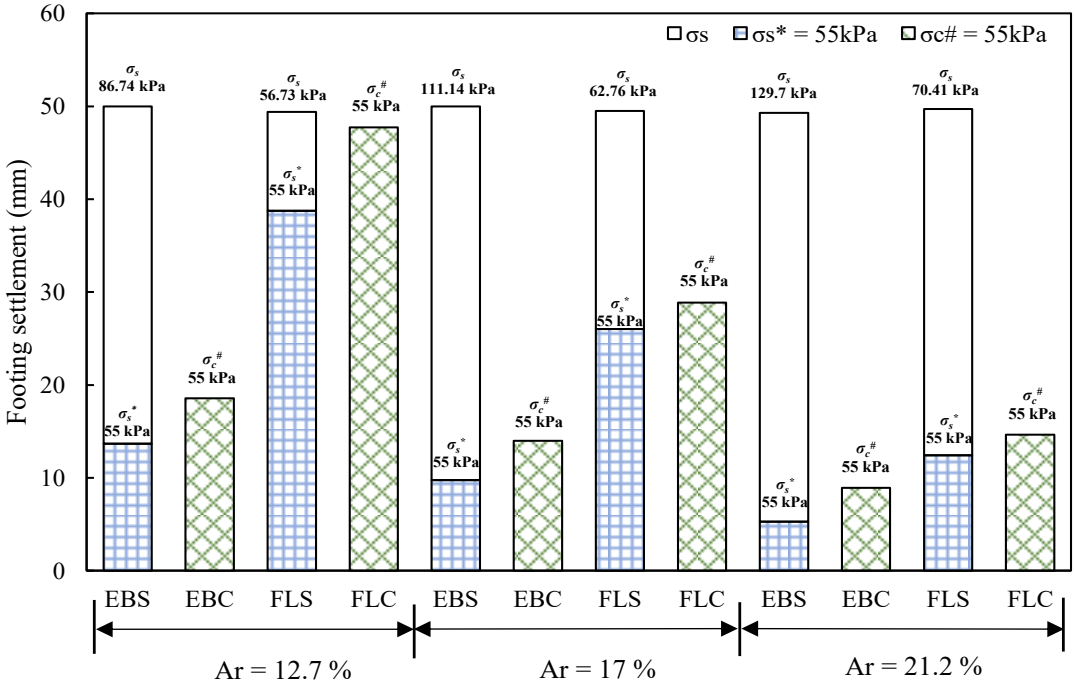

EBS: End-bearing under static load; EBC: End-bearing under cyclic load; FLS: Floating under static load; FLC: Floating under cyclic load. σ_s is the total stress level reached and the corresponding settlement achieved at failure during static loading.

\# settlement corresponding to cyclic stress (σ_c) of 55 kPa applied in 10,000 cycles.

* Settlement corresponding to σ_s of 55 kPa under static loading.

Fig. 6.12 Comparison of the footing settlement of the embankment model improved with end-bearing (l/h = 1) and floating (l/h = 0.75) GPSCs for A_r of 12.7%, 17% and 21.2% under static and cyclic loading.

6.3.3 Carbon Footprint Analysis and Cost Estimation

The term carbon footprint describes the total quantity of greenhouse gases (GHGs), mostly carbon dioxide (CO_2), that are released into the atmosphere as a result of human activity, both directly and indirectly. In order to mitigate climate change and its detrimental consequences on the environment, human health, and economy, reducing carbon footprints is crucial (Valente et al. 2022). More than 7% of carbon dioxide (CO_2), sulfur dioxide (SO_2), and nitrous oxide emissions are attributable to cement. Over 50% of the carbon dioxide released during the cement-making process originates

from the decarbonization of limestone, with the remaining portion coming from the combustion of fossil fuels (Davidovits 2008, Morsy et al. 2022).

The mix design for stabilizing 1 tonne of soil with OPC and GGBS-dolomite-based geopolymer is mentioned in Table 6.4. It should be noted that the sodium silicate used in this study was obtained in solution form [SiO_2 (28.1%), Na_2O (14%), H_2O (57.9%)] with SiO_2/Na_2O equal to 2. Therefore, the weight of SiO_2 and Na_2O is considered for carbon footprint calculation. Also, 8M NaOH solution was prepared using NaOH pellets, so the weight of solid NaOH is considered.

Table 6.4 Mix proportion of GGBS-dolomite-based geopolymer and OPC for dry soil of 1 tonne.

Materials	**Geopolymer**	**Cement**
GGBS (kg)	160	-
Dolomite (kg)	40	-
Sodium Hydroxide 8M solids (kg)	16	-
Sodium Silicate (kg)	150	-
Cement (kg)	-	200

For the CO_2 footprint analysis, the carbon coefficients of the materials were used to determine the amount of CO_2 emission per tonne. The life cycle inventory (LCI) of the materials used was taken from the previous literature and presented in Table 6.5 (Hu et al. 2023; Shao et al. 2023; Valente et al. 2022). NaOH has the highest and dolomite has the lowest carbon coefficient. The net CO_2 emission of geopolymer-stabilized soil using GGBS and dolomite as a binder and NaOH and Na_2SiO_3 as an alkali activator was compared with OPC-stabilized soil. The net CO_2 emission from materials used in geopolymerization and OPC is shown in Fig. 6.13. The utilization of GGBS-dolomite-

based geopolymer decreased the CO_2 emission by 33.73% compared to OPC-stabilized soft soil.

Table 6.5 CO_2 emission of cement and materials used in geopolymerization technique.

Material	**Cost ($/tonne)**	**CO_2 emission (t CO_2/tonne)**	**References for CO_2 emission**
OPC	161.4	0.903	Shao et al. 2023
GGBS	26.3	0.067	Valente et al. 2022
Dolomite	11.96	0.029	Hu et al. 2023
Sodium Hydroxide (NaOH)	298.93	1.915	Valente et al. 2022
Sodium Silicate (Na_2SiO_3)	149.46	1.222	Valente et al. 2022

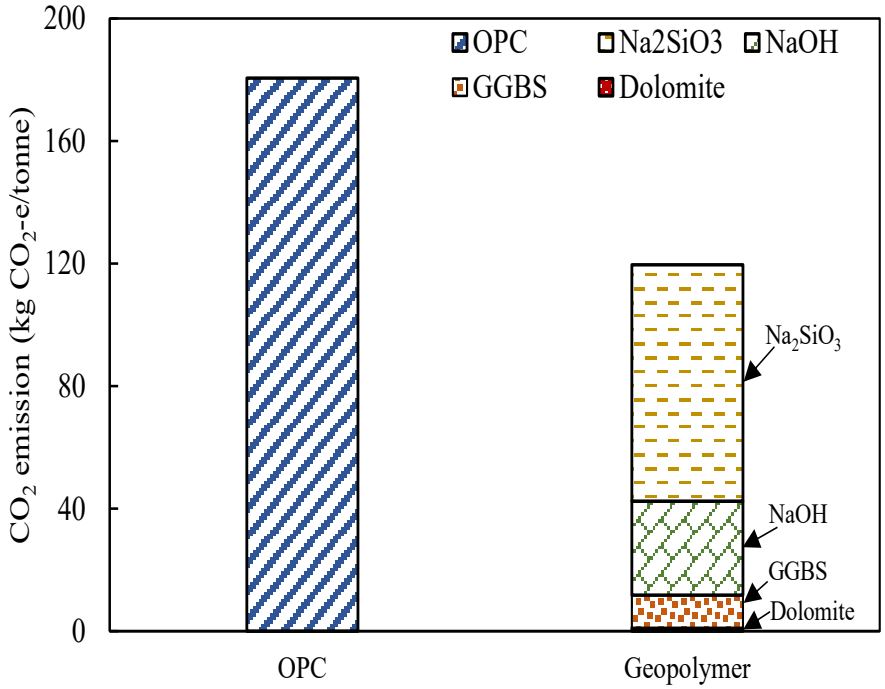

Fig. 6.13 Total CO_2 emission of OPC and GGBS-dolomite-based geopolymer stabilized soft soil.

The cost of a material is one of the primary factors that the building industry considers, in addition to its influence on the environment. Along with carbon footprint analysis, cost analysis of cement and geopolymer mix used to stabilize 1 tonne of soil was conducted in this study. The cost of the OPC and raw materials required to prepare the geopolymer mix are presented in Table 6.5. The cost of the raw materials might be different from the existing literature as it depends from country to country. The cost analysis was done on a material basis as the transportation cost is not included in the study. GGBS and dolomite are largely available in India, so the cost of the mentioned industrial waste by-products is relatively low. The cost of the geopolymer mainly depends on the NaOH and Na_2SiO_3 due to its higher cost (Bayraktar et al. 2024; Danish et al. 2023). The total cost of using OPC was 32.28 $/tonne, whereas the geopolymer mix was 31.88 $/tonne to stabilize 1 tonne of soil, as shown in Fig. 6.14.

Although the cost of geopolymer was a little lower than OPC, the carbon footprint of geopolymer was 33.73% lower than OPC, indicating a lower impact on the environment. Also, the compressive strength of geopolymer-treated soil was higher than OPC-treated soil with the same binder content of 20%. Future studies are recommended to reduce the amount of Na_2SiO_3 with some waste material of similar properties at less cost without compromising the compressive strength of geopolymer-treated soil. It can be concluded that geopolymer in the DSM technique is more effective and environmentally friendly, with higher compressive strength than the traditional binder.

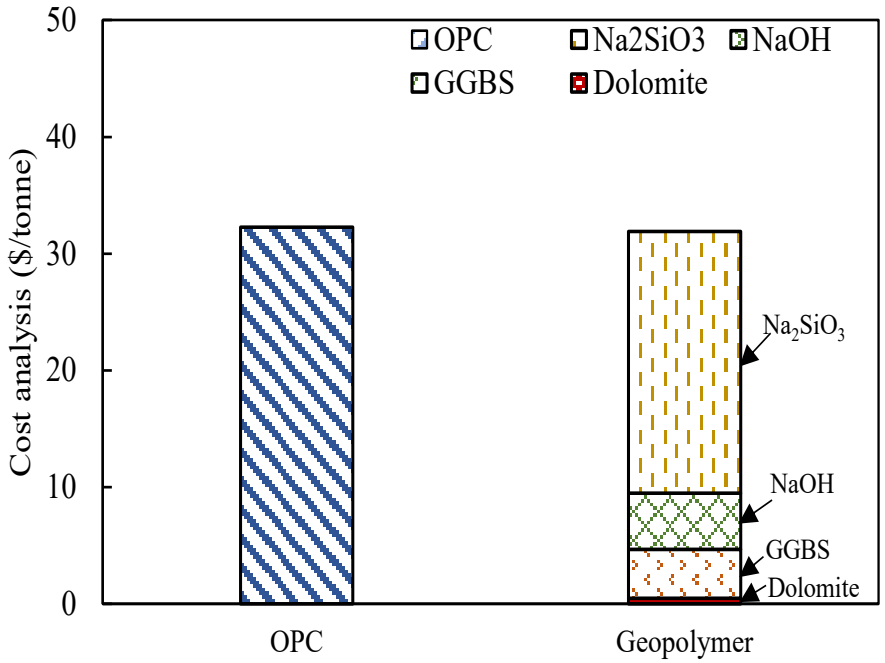

Fig. 6.14 Cost comparison of OPC and geopolymer.

6.4 Conclusion

This study aimed to study the behavior of end-bearing and floating GPSCs stabilized soft soil in an embankment model under static and cyclic loading. The cyclic loading was considered to simulate the cyclic stresses induced in transportation routes such as railways and roadways.

The installation of both end-bearing and floating GPSCs improved the bearing capacity and stiffness of the soft ground. While the installation of floating GPSCs enhanced the q_{ult} by 126.9% to 181.64%, the q_{ult} improved by 246.92% to 418.8% in the case of end-bearing GPSCs. Therefore, end-bearing GPSCs are more effective in minimizing soft ground settlement under static loading.

Both end-bearing and floating GPSCs improved ground showed 1.11 to 1.68 times higher settlement under cyclic loading compared to static loading, with the same rate of vertical stress under both loading conditions. Higher area replacement ratios are

required for floating GPSCs in order to improve load-bearing under both static and cyclic stress. The extra pore water pressure is effectively reduced by installing GPSCs in the soft soil. Under both static and cyclic loads, the SCR value increases as the A_r and *l/h* ratio increases.

Comparing the geopolymer binder to the traditional OPC binder, the carbon footprint analysis showed that the geopolymer binder offers potential savings of 33.73% on CO_2 emissions. Also, the cost of geopolymer was on the lower side compared to OPC.